






Fully Metallic Dual-Band Linear-to-Circular Polarizer for K/K_a-band

Johan Lundgren , Oskar Zetterstrom , *Student Member, IEEE*, Francisco Mesa , *Fellow, IEEE*, Nelson J. G. Fonseca , *Senior Member, IEEE*, and Oscar Quevedo-Teruel , *Senior Member, IEEE*

Abstract—A dual-band polarizer is presented that converts linear polarization into circular polarization with orthogonal handedness in the satcom bands 19.7–20.2 GHz and 29.5–30 GHz. The polarizer consists of three identical cascaded perforated metallic screens, whose perforations are periodically repeated crosses of two sizes. Unlike previously reported dual-band polarizers, our design is fully metallic, which results in low losses and makes it suitable for space applications. A prototype of the polarizer with 20×20 unit cells is manufactured, and the measurement results agree well with the simulated results. In the nominal satcom bands, the measured axial ratio and the insertion loss are better than 1.7 and 0.67 dB. In the bands 18.9–20.3 GHz and 29.1–30.1 GHz, the measured axial ratio and insertion loss are below 3 and 1 dB.

Index Terms—Circular polarization, dual-band polarizer, fully metallic, K/K_a-band, polarization conversion.

I. INTRODUCTION

ELECTROMAGNETIC waves with circular polarization (CP) play an important role in satellite and point-to-point communication. Compared to linear polarization (LP), communication using CP has the benefit that the transmitting and receiving antennas do not have to be aligned to maximize the transferred power [1]. Additionally, the polarization state of CP waves is not altered by the Faraday effect [2].

Electromagnetic waves with CP are generated from, e.g., helical antennas [1] or log-spiral antennas [3] with the corresponding excitation. In these antennas, the handedness of the spiral or helix determines the handedness of the CP. Consequently, these antennas cannot provide dual-band properties with orthogonal handedness in the two separate bands, a feature that is desired in

broadband satellite communications [4]. Alternatively, crossed dipoles fed in quadrature [5] and patch antennas [6] can be used to generate waves with CP. However, crossed dipoles and patch antennas are narrow-band and low-directive antennas, which makes them inadequate for some applications. Furthermore, patch antennas require supporting substrates that are lossy at millimeter-wave frequencies.

Alternatively, a polarizer can be used to transform LP to CP. This enables the use of antennas that inherently have LP in systems where CP is required. For instance, fully metallic aperture antennas integrated with an LP-to-CP polarizer can be used to produce cost-effective high gain CP antennas [7]–[12]. Additionally, a LP-to-CP polarizer readily generates orthogonal handedness in different bands.

A LP-to-CP polarizer can be treated as an anisotropic frequency selective surface (FSS), where the transmission characteristics are different depending on the polarization orientation of the incident wave. By cascading multiple FSS layers it is possible to improve the bandwidth [13] and the control of the scattering properties [14]. It has been demonstrated that three layers or more are required to design a LP-to-CP polarizer with no insertion loss (IL) at two frequencies [15]. A multimodal circuit model approach can be used to efficiently analyze FSSs, additionally providing physical insight into their operation [16]–[21].

Different types of LP-to-CP transmit polarizers have been proposed in the scientific literature. For instance, metal strip polarizers [15], [22] and meander-lines [23]–[28] photo-etched or printed on dielectric substrates have been designed for single-band applications. Moreover, a wideband multilayer single-band polarizer based on split-rings bisected by strips was proposed in [29]. Dual-band polarizers with orthogonal handedness of the polarization in the two bands have been presented [30], [31] and recently proposed for broadband satcom services [32]–[35]. The aforementioned designs require a mechanical support structure (usually a substrate), which is a source of losses at millimeter-wave frequencies. Alternatively, slot-based geometries can be employed. These structures can be made fully metallic and are, thus, suitable for high frequency applications [36]–[38].

In this letter, a slot-based dual-band polarizer is proposed for the K/K_a-band allocated to satellite broadband services. It consists of three perforated screens separated by an air gap. The perforations in each screen are made of two sets of periodically repeated cross-shaped slots, one set for each band. The slot-based geometry allows for a fully metallic implementation,

Manuscript received April 7, 2021; revised May 11, 2021; accepted May 12, 2021. Date of publication May 18, 2021; date of current version November 16, 2021. This work was supported in part by the Strategic Innovation Program Smarter Electronics System - A Joint Venture of Vinnova, Formas, and the Swedish Energy Agency, under Project High-Int 2019-02103. The work of Francisco Mesa was supported by the Spanish Government under the Salvador de Madariaga fellowship PRX19/00025 and Project TEC2017-84724-P. (*Corresponding author: Johan Lundgren.*)

Johan Lundgren, Oskar Zetterstrom, and Oscar Quevedo-Teruel are with the Division of Electromagnetic Engineering, KTH Royal Institute of Technology, 11428 Stockholm, Sweden (e-mail: jlu8@kth.se; oskarz@kth.se; oscarqt@kth.se).

Francisco Mesa is with the Departamento de Física Aplicada 1, E.T.S. de Ingeniería Informática, University of Seville, 41012 Seville, Spain (e-mail: mesa@us.es).

Nelson J. G. Fonseca is with the Antenna and Sub-Millimetre Waves Section, European Space Agency, 2200 AG Noordwijk, The Netherlands (e-mail: nelson.fonseca@esa.int).

Digital Object Identifier 10.1109/LAWP.2021.3081655

which results in a high efficiency. Additionally, by using three screens, we obtain a low IL in two separate bands with serviceable bandwidth. The operation in the different bands, and in particular the CP handedness, is nearly independently controlled. The polarizer converts LP into right-hand CP (RHCP) in the lower band (19.7–20.2 GHz) and the same LP into left-hand CP (LHCP) in the upper band (29.5–30 GHz). With a criteria of 3 dB to define the axial ratio (AR) bandwidth, the polarization conversion is extended over the bands 19.3–20.6 GHz and 28.8–30.3 GHz, respectively.

II. POLARIZER OPERATION PRINCIPLE

The E -field of a time-harmonic CP wave propagating in the $+z$ -direction can be written in terms of two orthogonal waves with LP as

$$\mathbf{E}^{\text{CP}} = E_0 e^{-jkz} \hat{\mathbf{x}} + E_0 e^{-j(kz \pm \pi/2)} \hat{\mathbf{y}} \quad (1)$$

where E_0 is the amplitude of the field, k is the wavenumber, and the $e^{j\omega t}$ -dependence is suppressed. The proposed polarizer presented in this letter operates by introducing the required $\pm\pi/2$ phase difference between two orthogonal LP impinging waves initially in-phase. In many cases, the feed antenna emits only waves with one LP. However, by tilting the feed $\delta = 45^\circ$ with respect to the polarizer, the incident waves at the polarizer is decomposed into two orthogonal components that are in-phase with equal magnitude. This concept is illustrated in Fig. 1, where the tilting angle δ is indicated and the impinging wave with LP is decomposed as

$$\mathbf{E}^{\text{i}} = E_0 e^{-jkz} \hat{\mathbf{x}} + E_0 e^{-jkz} \hat{\mathbf{y}}. \quad (2)$$

The performance of the polarizer is evaluated by considering the E -field transmitted through the polarizer. Decomposing the transmitted E -field into two orthogonal waves with LP gives

$$\mathbf{E}^{\text{t}} = (E_x \hat{\mathbf{x}} + E_y \hat{\mathbf{y}}) e^{-jkz} = (|E_x| e^{j\varphi_x} \hat{\mathbf{x}} + |E_y| e^{j\varphi_y} \hat{\mathbf{y}}) e^{-jkz} \quad (3)$$

and the transmission coefficient of an x -polarized (y -polarized) wave through the polarizer is defined as E_x/E_0 (E_y/E_0). It is desired to have low IL for both orthogonal polarizations, and in this letter, we target an IL below 1 dB. The phase difference between the two waves with orthogonal LP at the polarizer output is defined as

$$\Delta\varphi = \varphi_y - \varphi_x \quad (4)$$

where a phase difference of -90° results in conversion to RHCP and, a phase difference of $+90^\circ$ results in conversion to LHCP [39]. The AR of the transmitted wave is defined as [1]

$$\text{AR} = \left(\frac{|E_x|^2 + |E_y|^2 + \sqrt{a}}{|E_x|^2 + |E_y|^2 - \sqrt{a}} \right)^{1/2} \quad (5)$$

where a is given by

$$a = |E_x|^4 + |E_y|^4 + 2|E_x|^2|E_y|^2 \cos(2\Delta\varphi). \quad (6)$$

III. POLARIZER DESIGN

The unit cell of the proposed polarizer is illustrated in Fig. 1(a), where the gray area represents metal. In Fig. 1(b), the

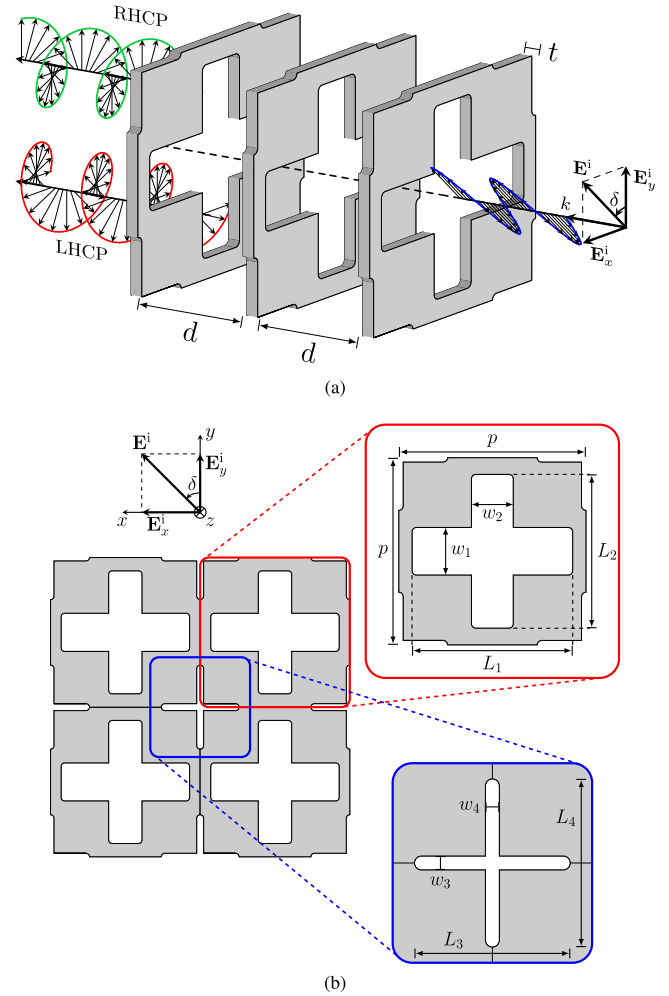


Fig. 1. (a) Unit cell of the proposed polarizer and illustration of the conversion between LP and CP. (b) 2×2 unit cells.

periodic arrangement of the unit cell is illustrated. The polarizer consists of three identical perforated screens. The perforations consist of two sets of crossed slot openings, one large and one small for the low and high frequency band, respectively. The dimensions of the horizontal (vertical) slots in the crosses mainly affect the transmission amplitude and phase of the y -polarized (x -polarized) waves, with the larger (smaller) crosses affecting primarily the response in the lower (higher) frequency band. By using different lengths of the two orthogonal slots for the same band, a phase shift is introduced between the two polarizations. If the vertical slot is slightly shorter (longer) than the horizontal, the horizontal polarization is leading (lagging) the vertical component and $\Delta\varphi$ becomes negative (positive). By tuning the slots for the two bands, an LHCP wave can be achieved in one band and an RHCP wave in the other.

The dimensions of the unit cell and distance between the layers are optimized to achieve an IL below 0.5 dB and an AR below 1 dB over the down-link (19.7–20.2 GHz) and the up-link (29.5–30 GHz) frequency bands for broadband satcom. These requirements are the main motivation for a multilayer design, since a single-layer design demonstrated to provide an AR bandwidth below 1 dB of less than 1% [36]. Furthermore,

TABLE I
DESIGN PARAMETERS OF THE POLARIZER

Parameter	p	t	L_1	L_2	L_3	L_4
Value (mm)	9.6	0.5	8.25	7.9	5.0	5.4
Parameter	d	w_1	w_2	w_3	w_4	
Value (mm)	3.2	2.45	2.15	0.45	0.45	

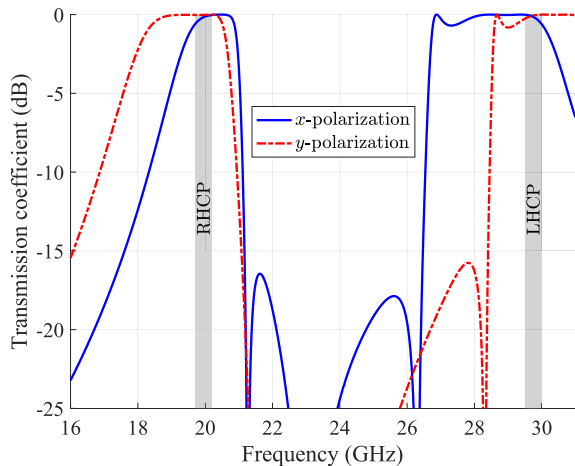


Fig. 2. Simulated transmission coefficient for two normally impinging orthogonal waves (LP). The shaded gray areas are the targeted satcom bands.

the periodicity of the unit cell is chosen so that grating lobes are avoided in the higher frequency band at normal incidence. This implies that the periodicity must be shorter than the wavelength corresponding to the highest frequency of operation (i.e., 30 GHz). However, this periodicity is also constrained by the lowest operating frequency that defines the size of the crossed slot opening. The dimensions of the polarizer are reported in Table I. To facilitate the manufacturing by water cutting, the inner corners of the slots are rounded with a radius of 0.225 mm.

IV. SIMULATION RESULTS OF THE POLARIZER

The structure in Fig. 1 is simulated using the frequency domain solver of CST Microwave Studio with periodic boundary conditions in the x - and y -directions [40]. The amplitude of the transmission coefficients for the two orthogonal LP waves under normal incidence are presented in Fig. 2. The transmission for both polarizations is above -0.61 dB in the nominal satcom bands from 19.7–20.2 GHz and 29.5–30 GHz. The phase difference $\Delta\varphi$ is presented in Fig. 3, where it can be observed that orthogonal handedness of the polarization is achieved in the two bands. The AR, calculated with (5), is presented in Fig. 4, showing values below 0.8 dB over the nominal satcom bands under consideration, and below 3 dB in the extended bands from 19.3–20.6 GHz and 28.8–30.3 GHz. The transmission coefficient for a single impinging wave with LP tilted 45° is illustrated in Fig. 5. The simulated conversion from LP to LHCP (RHCP) in the first (second) band is above -0.36 dB in the nominal satcom bands, and above -1 dB in the extended bands. The simulated

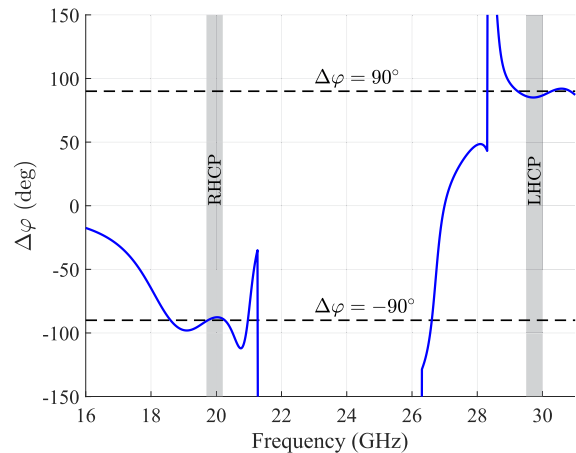


Fig. 3. Simulated transmission phase difference for two normally impinging orthogonal waves (LP).

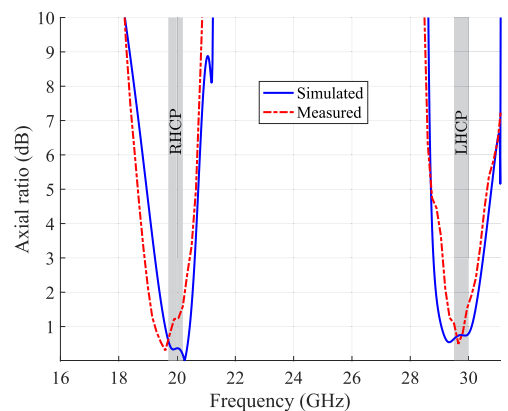


Fig. 4. Simulated and measured AR of the outgoing wave (CP) with a single impinging LP wave tilted 45° .

cross-polar transmission coefficient is below -27.5 dB in the nominal satcom bands, and below -15 dB in the extended bands.

V. MEASUREMENT RESULTS OF THE POLARIZER

A polarizer consisting of 20×20 unit cells is manufactured in aluminum using water cutting. The prototype is presented in Fig. 6, together with the measurement setup. Slabs of Rohacell HF 51 ($\epsilon_r = 1.06$ and $\tan \delta = 0.004$) are used to maintain the distance between the metallic screens. The polarizer is placed on a wooden stand centered between two horn antennas (with LP). The transmission between the two antennas is measured with the transmitting horn inclined 45° with respect to the main axes of the polarizer. Two orthogonal polarizations are sampled with the receiving antenna. The polarizer and the horn antennas are separated 80 cm. The distance is chosen to reduce the edge diffraction of the polarizer and still maintain a low phase error of the impinging wave. Absorbing materials were attached to the edges of the polarizer to mitigate the edge diffraction. However, no significant effect was observed, which indicates that the edge diffractions are small in the experimental setup.

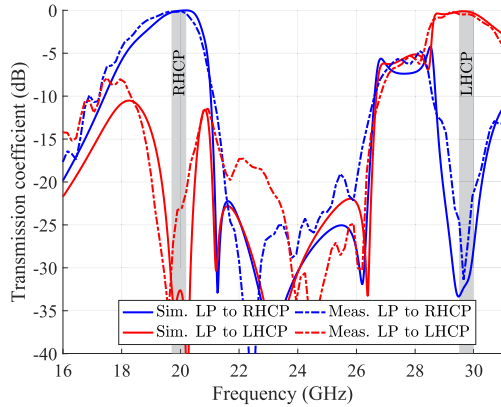


Fig. 5. Simulated and measured transmission coefficients for the polarization conversion.

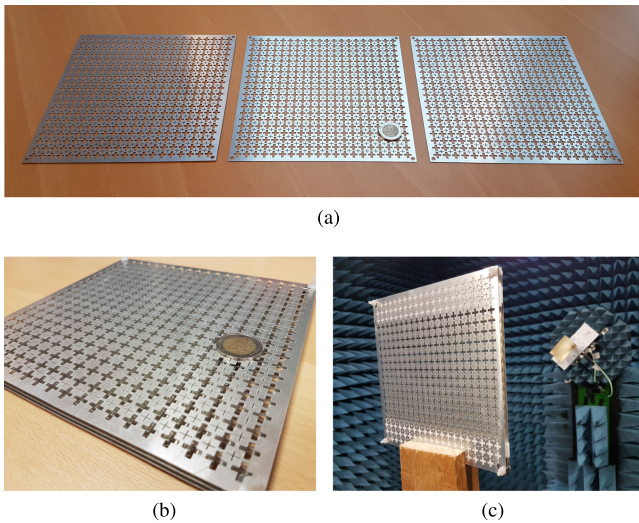


Fig. 6. (a) Manufactured screens. (b) Close-up view of the assembled prototype. A €2 coin is included for size-reference. (c) Measurement setup for the polarization conversion measurement.

The measured AR and transmission coefficient for the polarization conversion are presented in Figs. 4 and 5. The polarization conversion measurement is normalized to the measured linear-to-linear transmission between the two horn antennas without a polarizer in between. The measured conversion from LP to CP in the nominal satcom bands is above -0.67 dB with an AR below 1.7 dB, which corresponds to a cross-polar transmission coefficient below -21 dB. The measured conversion from LP to RHCP is above -1 dB from 18.9–20.3 GHz. The measured conversion from LP to LHCP is above -1 dB from 29.1–30.1 GHz. The measured AR is below 3 dB in these frequency bands. The simulations and measurements are in excellent agreement, apart from a 0.4 GHz frequency shift in the lower band. This shift is attributed to truncation effects due to the finite size of the prototype, which is more detrimental at the lower band.

In Table II, the presented polarizer is compared to previously reported dual-band LP-to-CP polarizers. In the present design, the measured AR is lower than the reference designs.

TABLE II
COMPARISON WITH REPORTED DUAL-BAND LP-TO-CP POLARIZERS

Reference	Center Frequencies (GHz)	IL (dB)	AR (dB)	Fractional Bandwidth (%)	Fully metallic
[30]	5.1/6.4	<6	<3	1.2/2	No
[31]	9.8/11.8	<4	-	-	No
[32]	19.95/29.75	<0.7	<2	2.5/1.7	No
[33]	18.5/29	<2	<3	29/12	No
[34]	19.95/29.75	<1.5	<2	2.5/1.7	No
[35]	20.1/29.55	<1	<3	21/5.8	No
This work	19.95/29.75	<0.7	<1.7	2.5/1.7	Yes

The measured IL is lower or equal to the reference designs. Importantly, the presented design is fully metallic. As a result, the low IL is expected to be maintained at even higher frequencies. Conversely, the reference polarizers require a mechanical supporting structure that introduces losses. These losses increase with frequency.

It is noted that the reference designs can have smaller unit cells due to the dielectrics, compared to the present polarizer. With smaller unit cells, the polarization transformation can be maintained at larger oblique incidence. Further investigations are aimed at improving the performance of fully metallic polarizers under oblique incidence.

VI. CONCLUSION

In this letter, a fully metallic dual-band polarizer is presented that converts LP into CP with orthogonal handedness in two bands, 19.7–20.2 GHz and 29.5–30 GHz. The polarizer consists of three identical perforated metallic screens that are separated by air gaps. The perforations consist of two interleaved periodic arrays of cross-shaped subwavelength apertures. The apertures have two sizes that perform the polarization conversion in one band each. A prototype consisting of 20×20 unit cells is manufactured and tested. The measured results in the finite structure agree well with the simulated results in the periodic environment. The measured IL is below 0.67 dB, with an AR below 1.7 dB in the considered bands. The polarizer has a measured IL below 1 dB and AR below 3 dB for LP to RHCP from 18.9–20.3 GHz and for LP to LHCP from 29.1–30.1 GHz. The polarizer may be integrated with aperture antennas suitable for mm-wave applications, such as ground segment satcom terminals.

ACKNOWLEDGMENT

The authors would like to thank J. Freiberg for his help during the measurement of the prototype.

REFERENCES

- [1] C. A. Balanis, *Antenna Theory: Analysis and Design*, 2nd ed. New York, NY, USA: Wiley, 2016.
- [2] R. C. Johnson and H. Jasik, *Antenna Engineering Handbook*, 4th ed. New York, NY, USA: McGraw-Hill, 2007.
- [3] J. Dyson, "The characteristics and design of the conical log-spiral antenna," *IEEE Trans. Antennas Propag.*, vol. AP-13, no. 4, pp. 488–499, Jul. 1965.

- [4] N. J. G. Fonseca and C. Manganot, "High-performance electrically thin dual-band polarizing reflective surface for broadband satellite applications," *IEEE Trans. Antennas Propag.*, vol. 64, no. 2, pp. 640–649, Feb. 2016.
- [5] B. Y. Toh, R. Cahill, and V. F. Fusco, "Understanding and measuring circular polarization," *IEEE Trans. Educ.*, vol. 46, no. 3, pp. 313–318, Aug. 2003.
- [6] P. C. Sharma and K. C. Gupta, "Analysis and optimized design of single feed circularly polarized microstrip antennas," *IEEE Trans. Antennas Propag.*, vol. AP-31, no. 6, pp. 949–955, Nov. 1983.
- [7] Q. Liao, N. Fonseca, and O. Quevedo-Teruel, "Compact multibeam fully metallic geodesic lens antenna based on non-Euclidian transformation optics," *IEEE Trans. Antennas Propag.*, vol. 66, no. 12, pp. 7383–7388, Dec. 2018.
- [8] O. Quevedo-Teruel, J. Miao, M. Mattsson, A. Algaba-Brazalez, M. Johansson, and L. Manholm, "Glide-symmetric fully metallic lüneburg lens for 5G communications at Ka-band," *IEEE Antennas Wireless Propag. Lett.*, vol. 17, no. 9, pp. 1588–1592, Sep. 2018.
- [9] O. Zetterstrom, E. Pucci, P. Padilla, L. Wang, and O. Quevedo-Teruel, "Low-dispersive leaky wave antennas for point-to-point high-throughput communications," *IEEE Trans. Antennas Propag.*, vol. 68, no. 3, pp. 1322–1331, Mar. 2019.
- [10] Q. Chen, O. Zetterstrom, E. Pucci, A. Palomares-Caballero, P. Padilla, and O. Quevedo-Teruel, "Glide-symmetric holey leaky-wave antenna with low dispersion for 60-point-to-point communications," *IEEE Trans. Antennas Propag.*, vol. 68, no. 3, pp. 1925–1936, Mar. 2020.
- [11] O. Dahlberg, G. Valerio, and O. Quevedo-Teruel, "Fully metallic flat lens based on locally twist-symmetric array of complementary split-ring resonators," *Symmetry*, vol. 11, no. 4, 2019, Art. no. 581.
- [12] N. J. G. Fonseca, Q. Liao, and O. Quevedo-Teruel, "Equivalent planar lens ray-tracing model to design modulated geodesic lenses using non-Euclidian transformation optics," *IEEE Trans. Antennas Propag.*, vol. 68, no. 5, pp. 3410–3422, May 2020.
- [13] B. A. Munk, *Frequency Selective Surfaces: Theory and Design*. New York, NY, USA: Wiley, 2000.
- [14] C. Pfeiffer and A. Grbic, "Bianisotropic metasurfaces for optimal polarization control: Analysis and synthesis," *Phys. Rev. Appl.*, vol. 2, no. 4, Oct. 2014, Art. no. 044011.
- [15] D. Lerner, "A wave polarization converter for circular polarization," *IEEE Trans. Antennas Propag.*, vol. AP-13, no. 1, pp. 3–7, Jan. 1965.
- [16] R. Rodríguez-Berral, F. Mesa, and F. Medina, "Analytical multimodal network approach for 2-D arrays of planar patches/apertures embedded in a layered medium," *IEEE Trans. Antennas Propag.*, vol. 63, no. 5, pp. 1969–1984, May 2015.
- [17] F. Mesa, M. García-Vigueras, F. Medina, R. Rodríguez-Berral, and J. R. Mosig, "Circuit-model analysis of frequency selective surfaces with scatterers of arbitrary geometry," *IEEE Antennas Wireless Propag. Lett.*, vol. 14, pp. 135–138, 2015.
- [18] F. Mesa, R. Rodríguez-Berral, M. García-Vigueras, F. Medina, and J. R. Mosig, "Simplified modal expansion to analyze frequency-selective surfaces: An equivalent circuit approach," *IEEE Trans. Antennas Propag.*, vol. 64, no. 3, pp. 1106–1111, Mar. 2016.
- [19] C. Molero, M. García-Vigueras, R. Rodríguez-Berral, F. Mesa, and N. Llombart, "Equivalent circuit approach for practical applications of meander-line gratings," *IEEE Antennas Wireless Propag. Lett.*, vol. 16, pp. 3088–3091, 2017.
- [20] F. Mesa, R. Rodríguez-Berral, M. García-Vigueras, and F. Medina, "Efficient hybrid full-wave/circuitual approach for stacks of frequency selective surfaces," *IEEE Antennas Wireless Propag. Lett.*, vol. 17, no. 10, pp. 1925–1929, Oct. 2018.
- [21] A. Alex-Amor, F. Mesa, Á. Palomares-Caballero, C. Molero, and P. Padilla, "Exploring the potentials of the multi-modal equivalent circuit approach for stacks of 2-D aperture arrays," *IEEE Trans. Antennas Propag.*, early access, Apr. 6, 2021, doi: [10.1109/TAP.2021.3070150](https://doi.org/10.1109/TAP.2021.3070150).
- [22] F. J. V. Sanchez and R. Pearson, "Electromagnetic wave polarizer screen," US Pat. 13/992628, Sep. 2013.
- [23] J. Epis, "Broadband antenna polarizer," US Pat. 3,754,271, Aug. 1973.
- [24] L. Young, L. Robinson, and C. Hacking, "Meander-line polarizer," *IEEE Trans. Antennas Propag.*, vol. 21, no. 3, pp. 376–378, May 1973.
- [25] R.-S. Chu and K.-M. Lee, "Analytical method of a multilayered meander-line polarizer plate with normal and oblique plane-wave incidence," *IEEE Trans. Antennas Propag.*, vol. AP-35, no. 6, pp. 652–661, Jun. 1987.
- [26] M.-A. Joyal and J.-J. Laurin, "Analysis and design of thin circular polarizers based on meander lines," *IEEE Trans. Antennas Propag.*, vol. 60, no. 6, pp. 3007–3011, Jun. 2012.
- [27] J. D. Baena, J. P. del Risco, A. P. Slobozhanyuk, S. B. Glybovski, and P. A. Belov, "Self-complementary metasurfaces for linear-to-circular polarization conversion," *Phys. Rev. B*, vol. 92, Dec. 2015, Art. no. 245413.
- [28] J. D. Baena, S. B. Glybovski, J. P. del Risco, A. P. Slobozhanyuk, and P. A. Belov, "Broadband and thin linear-to-circular polarizers based on self-complementary zigzag metasurfaces," *IEEE Trans. Antennas Propag.*, vol. 65, no. 8, pp. 4124–4133, Aug. 2017.
- [29] L. Martínez-López, J. Rodríguez-Cuevas, J. I. Martínez-López, and A. E. Martynyuk, "A multilayer circular polarizer based on bisected splitting frequency selective surfaces," *IEEE Antennas Wireless Propag. Lett.*, vol. 13, pp. 153–156, 2014.
- [30] M. Mutlu, A. E. Akosman, A. E. Serebryannikov, and E. Ozbay, "Asymmetric chiral metamaterial circular polarizer based on four u-shaped split ring resonators," *Opt. Lett.*, vol. 36, no. 9, pp. 1653–1655, May 2011.
- [31] H.-X. Xu, G.-M. Wang, M. Q. Qi, T. Cai, and T. J. Cui, "Compact dual-band circular polarizer using twisted hilbert-shaped chiral metamaterial," *Opt. Exp.*, vol. 21, no. 21, pp. 24912–24921, Oct. 2013.
- [32] P. Naseri, S. A. Matos, J. R. Costa, C. A. Fernandes, and N. J. G. Fonseca, "Dual-band dual-linear-to-circular polarization converter in transmission mode application to K/Ka-band satellite communications," *IEEE Trans. Antennas Propag.*, vol. 66, no. 12, pp. 7128–7137, Dec. 2018.
- [33] H. B. Wang and Y. J. Cheng, "Single-layer dual-band linear-to-circular polarization converter with wide axial ratio bandwidth and different polarization modes," *IEEE Trans. Antennas Propag.*, vol. 67, no. 6, pp. 4296–4301, Jun. 2019.
- [34] E. Arneri, F. Greco, L. Boccia, and G. Amendola, "A SIW-based polarization rotator with an application to linear-to-circular dual-band polarizers at K/K_a-band," *IEEE Trans. Antennas Propag.*, vol. 68, no. 5, pp. 3730–3738, May 2020.
- [35] M. Del Mastro, M. Ettore, and A. Grbic, "Dual-band, orthogonally-polarized LP-to-CP converter for SatCom applications," *IEEE Trans. Antennas Propag.*, vol. 68, no. 9, pp. 6764–6776, Sep. 2020.
- [36] S. Clendinning, R. Cahill, D. Zelenchuk, and V. Fusco, "Bandwidth optimization of linear to circular polarization converters based on slot FSS," *Microw. Opt. Technol. Lett.*, vol. 61, no. 5, pp. 1200–1207, 2019.
- [37] M. Euler, V. Fusco, R. Cahill, and R. Dickie, "Comparison of frequency-selective screen-based linear to circular split-ring polarisation converters," *Microw. Antennas Propag.*, vol. 4, no. 11, pp. 1764–1772, Nov. 2010.
- [38] M. Euler, V. Fusco, R. Cahill, and R. Dickie, "325 GHz single layer sub-millimeter wave FSS based split slot ring linear to circular polarization converter," *IEEE Trans. Antennas Propag.*, vol. 58, no. 7, pp. 2457–2459, Jul. 2010.
- [39] "ANSI/IEEE standard 149-1979," *IEEE Std. test procedure for antennas*, 1979.
- [40] DASSAULT SYSTÈMES, "CST Microwave Studio, version 2019." Accessed: Nov. 3, 2020. [Online]. Available: <http://www.cst.com/>